Transmutations, Radioactivity and Afterheat in a D-T-Tokamak Fusion Reactor

W.F. Vogelsang, G.L. Kulcinski, R.G. Lott, and T.Y. Sung

November 20, 1973

UWFDM-74

FUSION TECHNOLOGY INSTITUTE

UNIVERSITY OF WISCONSIN

MADISON WISCONSIN

Transmutations, Radioactivity and Afterheat in a D-T-Tokamak Fusion Reactor

W.F. Vogelsang, G.L. Kulcinski, R.G. Lott, and
T.Y. Sung

Fusion Technology Institute
University of Wisconsin
1500 Engineering Drive
Madison, WI 53706

http://fti.neep.wisc.edu

November 20, 1973

UWFDM-74

Transmutations, Radioactivity and Afterheat in a D-T Tokamak Fusion Reactor

by

W. F. Vogelsang
G. L. Kulcinski
R. G. Lott
T. K. Sung

November 20, 1973

FDM 74

University of Wisconsin

Abstract

Calculations have been performed to assess the effects of fast neutron induced transmutation reactions in the blanket region surrounding the plasma in a Tokamak fusion reactor. The production of both stable and radioactive isotopes is considered in three structural materials suggested for CTR's; 316 stainless steel, niobium-1% zirconium and vanadium-20% titanium. The results show that significant changes in the composition of the alloys will be produced along with the generation of large amounts of helium and radioactivity. Of the three alloys studied from the point of view of chemical changes, radioactivity and afterheat, the vanadium-20% titanium alloy appears to be most favored followed by 316 stainless steel and niobium-1% zirconium.

Introduction

It is quite evident that the structural components of a D-T fusion reactor will be exposed to very intense high energy neutron fluxes[1,2]. The neutrons can interact with the various isotopes in the materials to cause transmutations which in turn can alter the mechanical and physical properties of a metal. Quite often the new isotopes are radioactive and decay away with half lives ranging from a few seconds to thousands of years. The energy released during the decay of the radioactive isotopes must also be considered from the standpoint of afterheat in the reactor structure. All three of the above phenomena take place in fission as well as fusion reactors. However, certain transmutation rates are higher in fusion systems because of the higher neutron energy associated with D-T reactions (~14 MeV) versus fission reactions (~1-2 MeV).

The object of this paper is to investigate the transmutations, radioactivity and afterheat associated with three alloys of current interest to the CTR (Controlled Thermonuclear Reactor) community; 316 stainless steel, vanadium-20% titanium and niobium-1% zirconium. In order to obtain quantitative information, it was necessary to use the neutron spectra and geometrical factors associated with a current reactor design. We have chosen the University of Wisconsin Tokamak Reactor Design, UWMAK-I[1] as the model for this system. A previous study of the radioactivity and afterheat of a D-T Tokamak reactor has been made by Steiner[3]. A study of this nature is dependent on the details of the reactor design and the method of calculating the neutron fluxes and reaction rates. This work treats several materials of interest for blanket structure in a self consistent way for the

UWMAK-I design and is therefore strictly speaking only valid for this reactor. The results do give an indication of whay may be expected in other Tokamak reactors when spectral and power level differences are taken into account.

Calculational Procedures

UWMAK-I is a 5000 Mw_{th} device with a lithium cooled blanket utilizing 316 SS as the first wall and the structure in the blanket. Some of the characteristics are given in Table I. A schematic drawing of the regions of the blanket is shown in Figure 1. The transmutation calculations will concentrate on the first wall where the problems are the most severe while activity and afterheat calculations will include the remainder of the blanket as well.

The neutron spectra at various points throughout the blanket of UWMAK-I have been calculated using the ANISN computer code. The details of the calculation are described in reference 1. The neutron spectrum at the first wall is shown in Figure 2. The spectra from FTR and EBR-II are shown in the same figure for comparison only. The reaction cross sections used with these fluxes were taken from ENDF/B-III when available and processed by the MACK[4] code. For those isotopes or reactions not on ENDF tapes, the cross sections were estimated from BNL 325 or other sources[5]. For the niobium calculations, the cross sections were taken from the suggestions of Steiner[3]. In calculating the activity or transmutations, successive neutron capture by the product nuclei were not considered except for a double capture in ^{58}Ni and for some particular situations in the Nb-1Zr system. This approach was taken because of the relatively low flux in this design which makes double capture less important and because of the complexity of the isotope chains in stainless steel and because in some cases of a lack of cross sections for the radioactive nuclei. The basic UWMAK-I

Table I

Parameters of UWMAK-I

Power - - 5000 Mw_{th} (1500 MW_e)

Aspect Ratio - - 2.6 (R = 13 m, a = 5 m)

Divertor - Poloidal, Double Null

Wall loading - - 1.25 Mw/m^2

Structural Material - - - 316 SS

Coolant - - - - Li (500°C Max)

First wall life - - - 2 years

Magnets- - - Superconducting (Fully Stabilized)

B_t^o = 38 kG, B_t^{max} = 86 kG

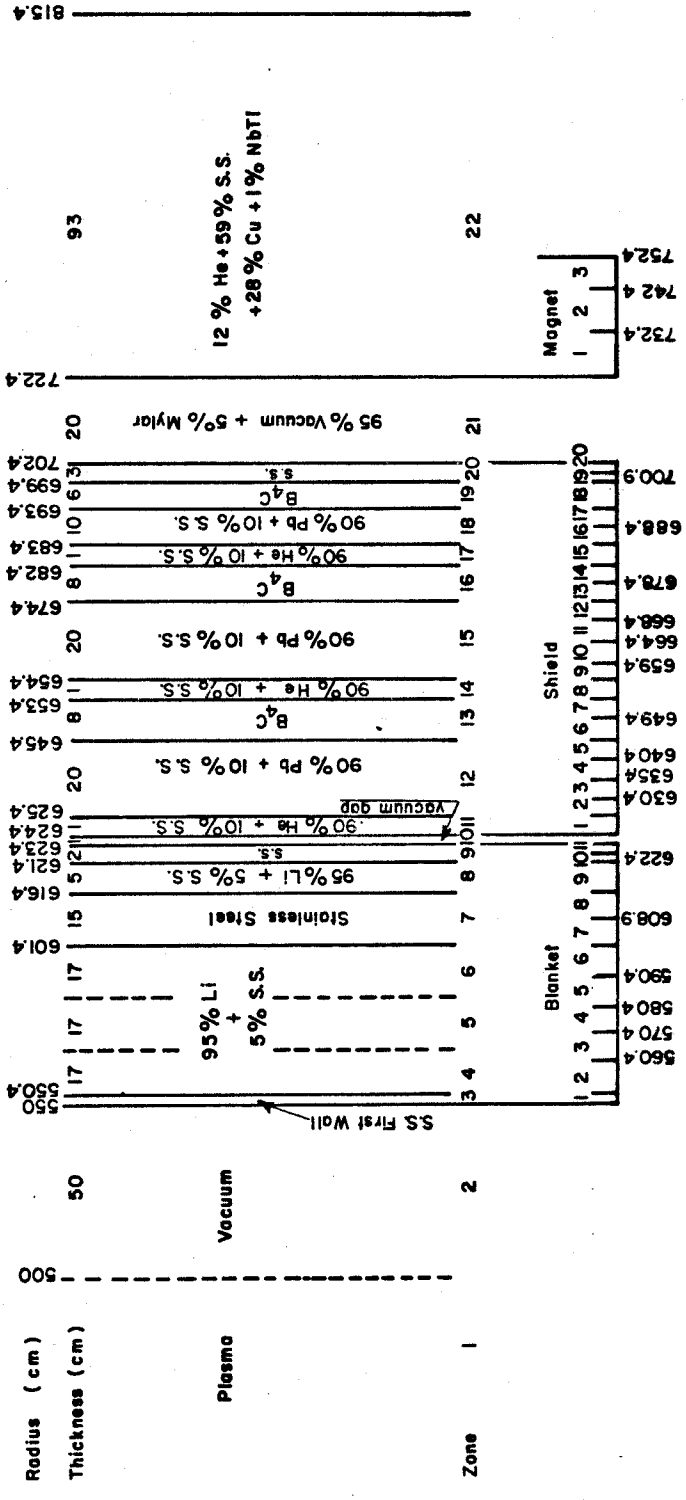
Radius (cm)
Thickness (cm)
Zone
Plasma
Vacuum
S.S. First Wall
95% Li + 5% S.S.
Stainless Steel
95% Li + 5% S.S.
s.s.
90% He + 10% S.S.
Vacuum gap
90% Pb + 10% S.S.
B4C
90% He + 10% S.S.
90% Pb + 10% S.S.
B4C
90% He + 10% S.S.
B4C
90% Pb + 10% S.S.
s.s.
95% Vacuum + 5% Mylar
12% He + 59% S.S. + 28% Cu + 1% NbTi
Blanket
Shield
Magnet
560.4
570.4
580.4
590.4
608.9
622.4
630.4
635.4
640.4
649.4
659.4
664.4
668.4
678.4
688.4
700.9
732.4
742.4
752.4
815.4

FIGURE 1

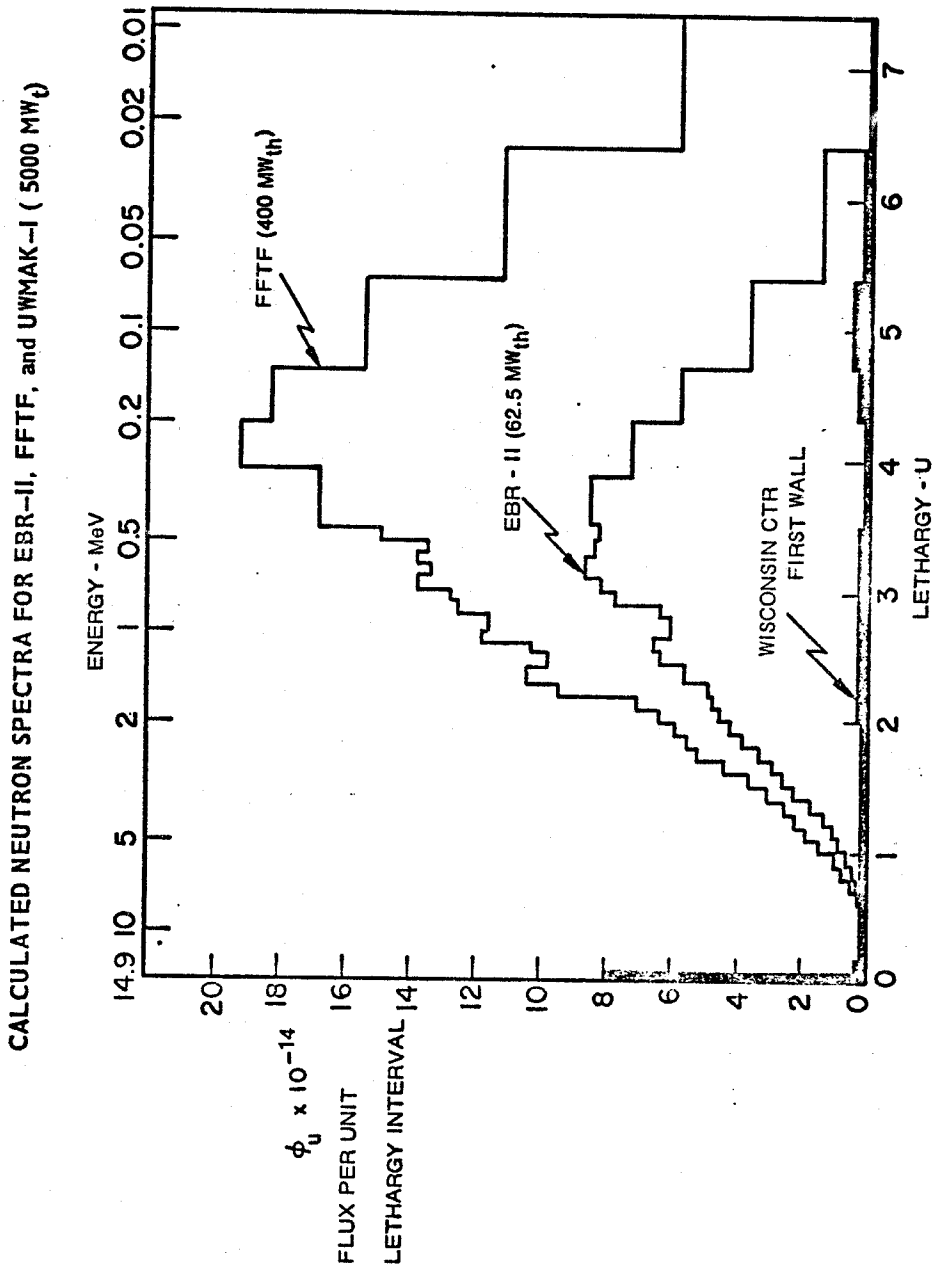
CALCULATED NEUTRON SPECTRA FOR EBR-II, FFTF, and UWMAK-I (5000 MWt)
ENERGY - MeV
14.9 10 5 2 1 0.5 0.2 0.1 0.05 0.02 0.01
FFTF (400 MWth)
EBR - II (62.5 MWth)
WISCONSIN CTR
FIRST WALL
LETHARGY - U
0 1 2 3 4 5 6 7
FLUX PER UNIT
LETHARGY INTERVAL
φu x 10-14
0 2 4 6 8 10 12 14 16 18 20

Figure 2

design utilized 316 SS as the first wall and structure material. Two alternate blanket materials Nb-1Zr and V-20Ti were also considered. In both cases, a one to one volume substitution was made for the stainless steel in the first wall (see Figure 1) and the 50 cm region immediately adjacent to the first wall. The remaining regions of what is defined as blanket, i.e. 23 cm of 316 SS and lithium were left unaltered. The neutron spectrum used was that of the 316 SS-Li blanket in all cases. Since the bulk of the material in the blanket region is lithium, the energy distribution and spatial dependence of the neutron flux is determined largely by the lithium rather than by the structure. Thus, the neutron flux is not a strong function of the structural material in UWMAK-I and need not be recalculated for each new material. Past experience has shown this approach gives results within 10% which, considering the accuracy of the cross sections used, is adequate for this work.

Transmutation Considerations

The production of transmutations can be conveniently divided into two areas, gaseous and non-gaseous products. Each of these topics will be treated separately.

Non-Gaseous Products

A summary of the major transmutation reactions in three potential CTR materials, 316 SS, V-20Ti and Nb-1Zr is given in Table II. Changes which amount to <100 ppm have been omitted for conciseness. The results include the production (or depletion) rate in amys [atomic parts per million per megawatt per $(\text{meter})^2$ per year] and only the reactions in the first wall are reported here. Similar transmutations take place in the blanket region (see Figure 1), but at a much reduced rate.

The most striking effect in 316 SS is the large increase in manganese content over a thirty year exposure. The manganese content increases by over a factor of three to ~6.4 atomic percent. There are equally large percentage increases in the titanium and vanadium composition of the steel. The largest change occurs for titanium which goes from 0.0115 atomic % to 0.18 atomic %, an increase by a factor of almost 16. There are corresponding decreases in the iron (62.3 to 58%) and in nickel (14 to 13.3%) content.

It is not clear at this time what such changes mean in a complex alloy like 316 SS. The change in iron and nickel are within composition limits for 316 SS but the increase in manganese content might make the steel behave more like a 200 series alloy than a 300 series alloy. In any case, manganese is an austenite stabilizer which should more than offset the loss of nickel. The increase in titanium content would make the steel appear more like a type 321 and the increase in V may produce a steel with properties similar to type 347. The effect of these elements on the carbide precipitation, and its subsequent effect on swelling or mechanical properties should be investigated.

It is also noted that if the first wall of the UWMAK-I blanket is changed every two years as has been suggested[2], then the alloy changes due to transmutations in 316 SS should present no particular problems.

The chemical changes in V-20Ti appear to be minimal and of a nature which should not cause a significant change in mechanical or physical properties. Furthermore, the small amount of scandium

Table II

Summary of Major Transmutation Effects in the First Wall of UWMAK-I(a

Element	Original Composition(at %)	Transmutation Rate appm per MW/m^2 per year	Composition-at % 2 yrs.	10 yrs.	30 yrs.
		316 SS			
Fe	62.6	-1224	62.3	61.1	58.0
Ni	14	- 177	14	13.8	13.3
Mn	2	+1160	2.3	3.5	6.4
Ti	0.012	+ 45	0.023	0.068	0.18
V	0.22	+ 177	0.26	0.44	0.88
		V-20Ti			
V	79.5	- 162	79.5	79.3	78.9
Ti	20	+ 53	20	20	20
Cr	0.002	+ 99	0.027	0.130	0.37
Sc	Negligible	+ 9	0.0023	0.011	0.034
		Nb-1Zr			
Nb	98.7	-1485	98.3	96.9	93.2
Zr	1.0	+1473	1.37	2.84	6.51
Y	Negligible	+ 12	0.0029	0.015	0.044

(a Wall loading 1.25 MW/m^2.

generated (<0.04%) is not expected to have a significant effect on this alloy. It, therefore, appears that there are no significant wall loading limitations due to transmutations for V-20Ti in a reactor like UWMAK-I up to perhaps 10 MW/m^2 for 30 years.

The situation for Nb-1Zr is not as optimistic as for the other two alloys considered in this study. The main problem stems from the high zirconium production rate in niobium. It can be seen from Table II that over 5 atomic percent of zirconium, in addition to the initial 1% zirconium would be generated in the first wall during a 30 year exposure. This additional zirconium could cause two problems. First, it tends to reduce the ductility of niobium[6]. Second, the solubility limit of zirconium in niobium is ~15 atomic percent at T <600°C[7]. The precipitation of second phase particles beyond this concentration could cause further reductions in ductility. One rather definite integral wall loading limitation could be set on niobium alloys; that is, the zirconium concentration should not exceed 15% during the life time of the component. This would restrict the integral wall loading in UWMAK-I to ~110 MW-years per m^2 from transmutations considerations.

Gaseous Production

A summary of the major contributors to gas production in the alloys considered here is given in Table III. Only those elements which make significant contributions were considered.

The most striking feature about gas production in 316 SS is the magnitude; 238 amys of helium and 509 amys of hydrogen. This helium production rate is ~4 to 9 times higher than in V-20Ti and Nb-1Zr respectively.

Table III

Summary of the Major Contributors to the Gas Production in Materials for UWMAK-I First Wall

Element	Original Concentration[a] at %	amys appm/MW/m^2/year He	H	Atomic % of total[b] He	H
		316 SS			
Fe	62.6	154	230	65	45
Cr	18	35	64	15	13
Ni	14	23[c]	184	10	36
		0.03[d]	-	0.01	-
Mn	2	2.6	8	1	2
Si	1.5	13	18	5	4
C	0.28	9.3	N	4	N
Cu	0.1	0.1	4	N	1
	Total[e]	238	509		
		V-20Ti			
V	79.5	47	94	88	52
Ti	20	3.3	85	6	47
O	0.26	1.0	0.3	2	0.2
C	0.06	2.1	N	3	N
	Total[e]	53.5	181		
		Nb-1Zr			
Nb	98.7	27	75	96	98
Zr	1	0.1	0.9	0.3	1
C	0.03	0.9	N	3	N
	Total[e]	28.7	76		

(a Concentration may not add up to 100% because some elements were omitted for this table.
(b Atomic % may not total 100% due to omission of some elements in this table.
(c Threshold (n,α) only
(d Helium from Ni-59 after 2 year operation
(e Total includes all gas produced even by those elements omitted from this table
N = negligible

The major contributor to helium production in 316 SS is iron (65%) as would be expected but it is noticed that silicon and carbon produce disproportionate amounts of helium. Silicon accounts for ~3 times the amount that would be expected from its concentration in the alloy (5% of the helium vs 1.5% of the atomic concentration) and carbon produces almost 14 times as much. Wehn all of the impurities are included in helium production it is found that they account for ~10% of the helium produced in 316 SS.

It has been known for some time that anomalous helium production occurs in Ni because of the ^{58}Ni (n,γ) ^{59}Ni (n,α) reaction sequence[8]. Therefore, calculations were performed to test how important the nickel-59 reaction is to helium production in the UWMAK-I spectrum. Ignoring the burnout of nickel-59 atoms, the number of nickel-59 atoms as a function of time, N^{59}, due to a concentration of N^{58} nickel-58 atoms undergoing (n,γ) reaction with a cross section σ^{γ} is

$$N^{59}(t) = \sum_i N^{58} \sigma_i^{\gamma} \phi_i t, \qquad (1)$$

where ϕ_i is the neutron flux in the i^{th} energy group. The number of helium atoms, N^{He}, produced in time T, is then:

$$N^{He} = \int_o^T \sum_j N^{59}(t)\sigma_j^{\alpha}\phi_j dt = \frac{N^{58}T^2}{2} \sum_j \sum_i \sigma_i^{\gamma}\sigma_j^{\alpha}\phi_i\phi_j, \qquad (2)$$

where σ^{α} is the (n,α) cross section for nickel-59. A more precise treatment would show that as the nickel-59 concentration approached steady state, N^{He} would be proportional to T, rather than T^2 which means the results presented will give a pessismistic estimate of helium production. The results of this calculation are shown in Figure 3, for three different

positions in the reactor. The (n,α) cross section of Kirouac[8] were used.

The helium produced from the nickel-59 reactions is a very small fraction of the total helium produced in the first wall, amounting to only 0.2% over a period of 30 years. This percentage increases to 0.6% at 34 cm from the first wall because the neutron spectrum is softer. A softer spectrum would increase Ni-59 production while at the same time reduce the helium resulting from threshold reactions. It is therefore concluded that the production of He from ^{59}Ni can safely be ignored in UWMAK-I blanket calculations.

The production of hydrogen in 316 SS is strongly influenced by Ni which produces over 2 times as much as its concentration would indicate. Impurity contributions are somewhat less than in the case of helium, but still a significant percentage of the total amount (~7%).

It is noted that the helium production in the V-20Ti alloy is dominated by V (88%) and there is a significant contribution from the oxygen and carbon impurities. Hydrogen production in that alloy is about evenly divided between V and Ti, the titanium tending to overproduce by a factor of ~2.5.

Finally, both the helium and hydrogen production in Nb-1Zr is dominated by Nb as might be expected. A disproportionate contribution from carbon is also noted here, being a factor of 100 more than its initial concentration would indicate.

Figure 4 shows how the helium contents of these alloys will increase as a function of irradiation time and is rather self explanatory. It is quite obvious that a thousand ppm of helium can be generated in a relatively short time in 316 SS, ~3 years. It takes ~17-18 years to reach the same helium content in V-20Ti and almost 30 years is required

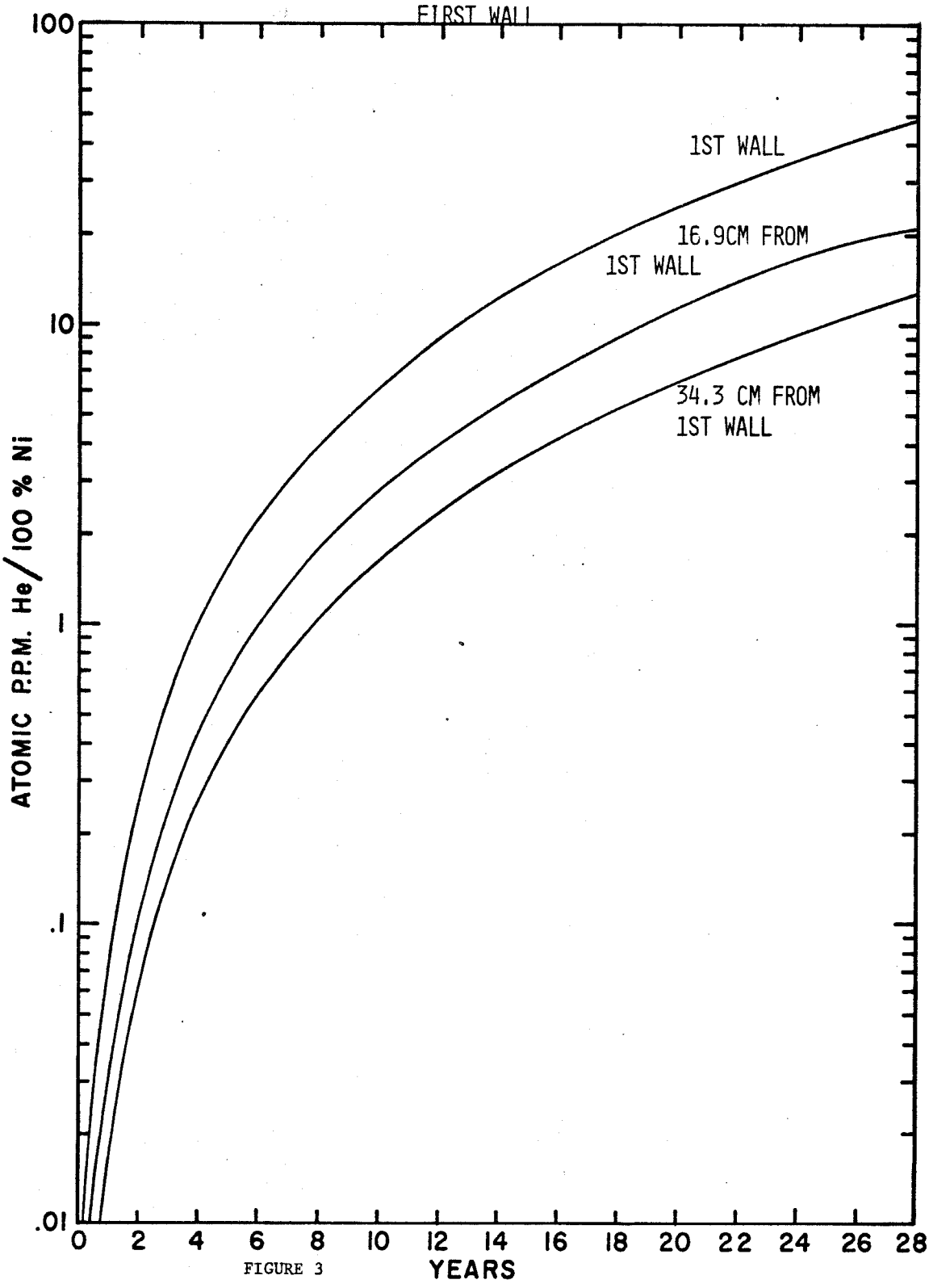
FIRST WALL
100
10
1
.1
.01
ATOMIC P.P.M. He/100 % Ni
1ST WALL
16.9CM FROM
1ST WALL
34.3 CM FROM
1ST WALL
0
2
4
6
8
10
12
14
16
18
20
22
24
26
28
YEARS

FIGURE 3

to produce 1000 appm helium in Nb-1Zr. The effect of such large amounts of helium are unknown at the present time but would be expected to severly embrittle the alloy at high irradiation temperatures, such as >600°C for 316 SS. Similar problems will occur for V-20Ti and Nb-1Zr alloys but at much higher temperatures.

Radioactivity

The radioactivity of the blanket for the three structural materials, 316 SS, Nb-1Zr and V-20Ti were calculated as a function of operating time and time after shutdown as described earlier. The reactions considered are shown in Table IV. The results will be expressed in total curies thus treating all isotopes equally.

There are three areas associated with the radioactivity of the blanket which are of particular interest. They are 1) the buildup of activity during operation 2) the decay of the activity following shutdown and 3) the hazard potential of the radioactivity. These are treated in the following sections.

Time Dependence of Radioactivity Generation

The radioactivity of the entire blanket as a function of time of operation is shown in Figure 5. Considering 316 SS as the base case, the most obvious feature is that the activity rises quite rapidly after startup, reaching 10^9 curies within two hours and rising to ~4 x 10^9 curies after two years. Thereafter, the rise is relatively slow such that after 40 years of continuous operation the activity would approach 6 x 10^9 curies. In considering the activity of the alternate systems, the qualitative features are similar, i.e. a relatively rapid initial rise followed by a much slower increase. While the activities of the blanket materials are of the same order of magnitude, there are some striking quantitative differences.

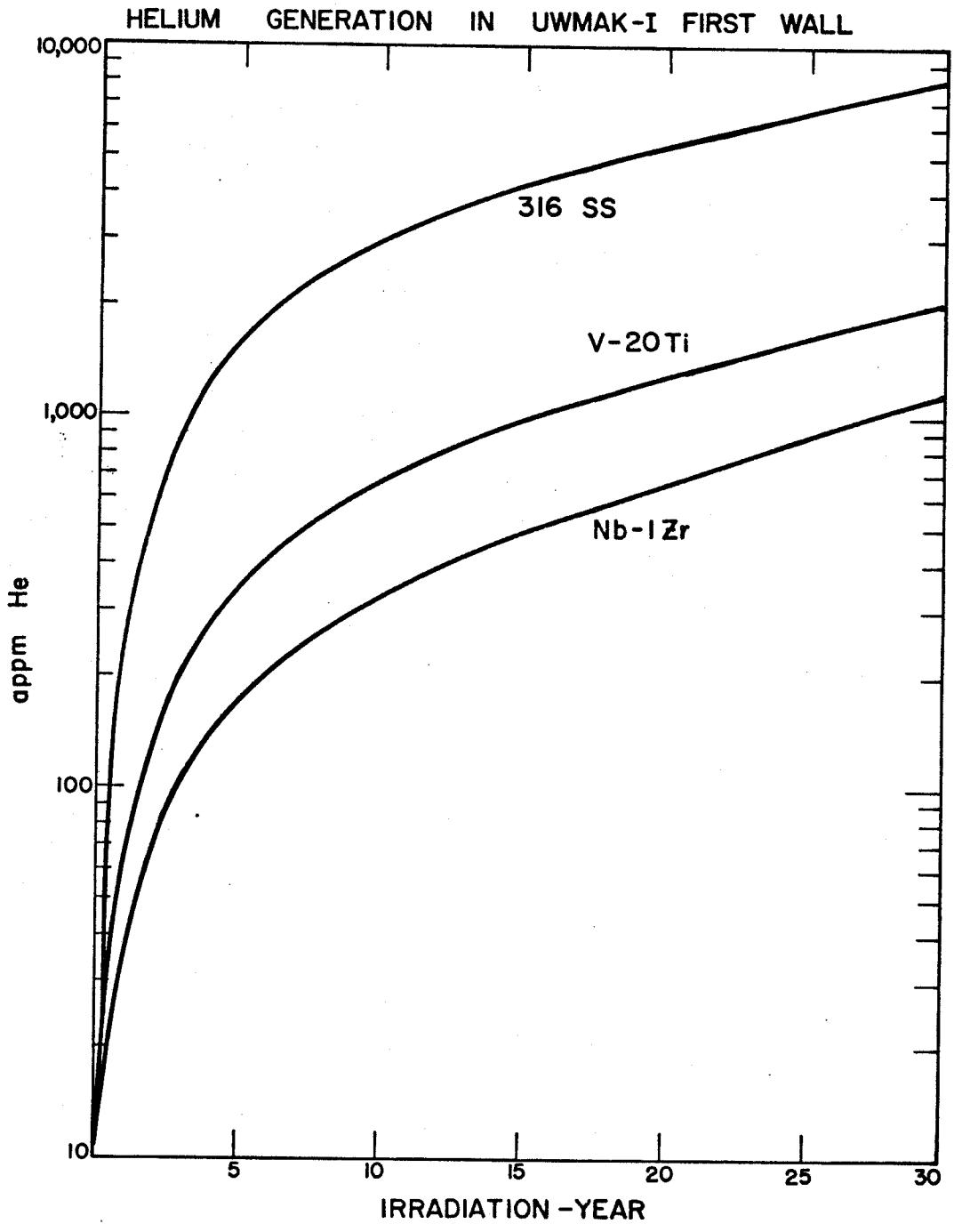
HELIUM GENERATION IN UWMAK-I FIRST WALL
10,000
1,000
100
10
appm He
316 SS
V-20Ti
Nb-1Zr
5
10
15
20
25
30
IRRADIATION -YEAR

FIGURE 4

The activity of the Nb-1Zr system is significantly larger than that of either the 316 SS of the V-20Ti system. The ratio of activity for Nb-1Zr to 316 SS is as high as a factor of four for operating times of a week of so. On the other hand, the activity of the V-20Ti system, while initially slightly larger than that of the 316 SS system, remains relatively constant after the first week and after twenty years of operation is less than one-half that of 316 SS. These features stem from the relative contributions of short and long lived isotopes. For the V-20Ti system there is only one relatively long lived isotope(^{45}Ca) as compared to SS which has several (Table V).

Time Dependence of Radioactive Decay

The radioactive decay in curies per watt of the first wall and lithium bearing regions of the blanket following a ten year operating time is shown in Figure 6. Considering 316 SS first, the predominant features are the high intital activities (~1 curie/watt or 5×10^9 curies total) and the relatively slow decay. The time for a reduction in activity by an order of magnitude is approximately ten years.

The activity in the time period for ten to thirty years is dominated by ^{60}Co ($T_{1/2}$ = 5.24 yr) and ^{55}Fe ($T_{1/2}$ = 2.4 yr). At longer times the residual activity is due to ^{63}Ni ($T_{1/2}$ = 92 yr). At 200 years for example, the total activity from the first wall is 350 curies corresponding to a density of only 0.031 millicuries/cm^3 of stainless steel.

The Nb-1Zr system activity is initially greater than that of the SS system by a factor of ~2.5. However, the initial decay is rapid enough so that after 1-2 weeks the activity is below that of 316 SS, dropping by a factor of 10 in about 10 weeks. At long times (~20 yrs)

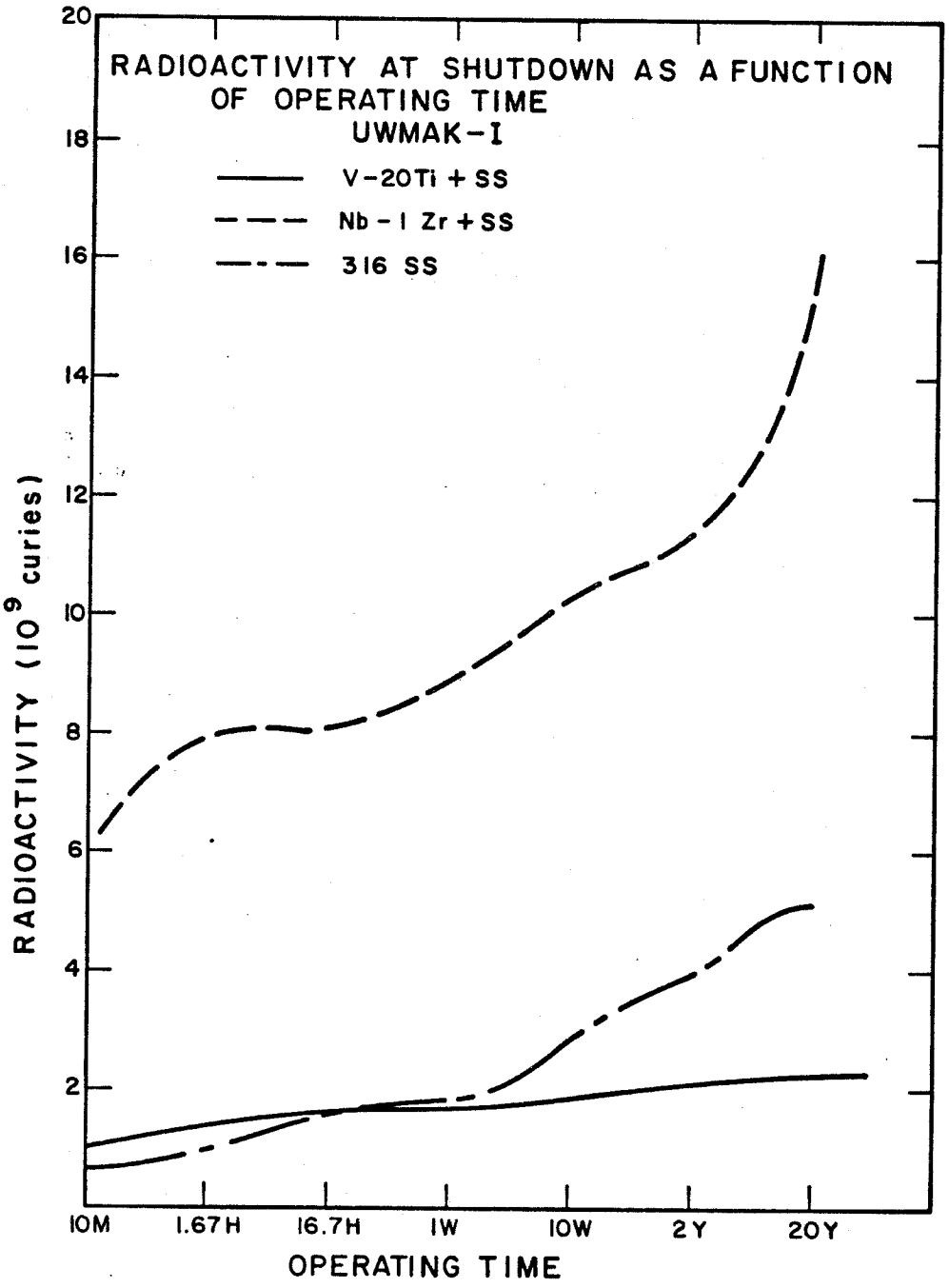
RADIOACTIVITY AT SHUTDOWN AS A FUNCTION OF OPERATING TIME
UWMAK-I
V-20Ti + SS
Nb - 1 Zr + SS
316 SS
RADIOACTIVITY (10^9 curies)
20
18
16
14
12
10
8
6
4
2
10M
1.67H
16.7H
1W
10W
2Y
20Y
OPERATING TIME

FIGURE 5

Table IV

Reactions Considered for Radioactivity Calculations

316 SS

^{28}Si (n,p),(n,α)
^{29}Si (n,p),(n,α)
^{30}Si (n,α),(n,p),(n,γ)
^{50}Cr (n,np),(n,2n),(n,γ)(n,p)
^{52}Cr (n,p),(n,2n),(n,γ)
^{53}Cr (n,np),(n,p),(n,γ)
^{55}Mn (n,α),(n,p),(n,2n),(n,nα),(n,γ)
^{54}Fe (n,α),(n,p),(n,2n),(n,np),(n,γ)
^{56}Fe (n,α),(n,np),(n,p),(n,2n),(n,γ)
^{57}Fe (n,p),(n,np),(n,γ)
^{58}Fe (n,α),(n,p),(n,γ)
^{58}Ni (n,nα), (n,α),(n,np),(n,p),(n,2n)
^{60}Ni (n,α),(n,p),(n,np)
^{61}Ni (n,α), (n,np),(n,p)
^{62}Ni (n,α),(n,np),(n,p)
^{64}Ni (n,np),n,p),(n,γ)

Nb-1Zr

^{90}Zr (n,p),(n,2n),(n,γ)
^{91}Zr (n,p),(n,γ)
^{92}Zr (n,γ)
^{94}Zr (n,α),(n,p),(n,γ)
^{93}Nb (n,2n),(n,p),(n,α),(n,n'),(n,γ)
^{94}Nb (n,γ)

V-20Ti

^{50}V (n,α),(n,2n),(n,p)
^{51}V (n,α),(n,p),(n,2),(n,2n)
^{46}Ti (n,p),(n,2n)
^{47}Ti (n,p),(n,np)
^{48}Ti (n,p),(n,α),(n,np)
^{49}Ti (n,p),(n,np)
^{50}Ti (n,p),(n,γ)

the principal contribution is from ^{94}Nb ($T_{1/2} \cong 20{,}000$ years) and the activity is greater than that of the SS system.

The V-20Ti system has an initial activity less than half that of the SS system. The relatively short lived isotopes in the activated vanadium die away quickly with a reduction by a factor of ten taking less than a week and a reduction by a factor of one hundred requiring ~20 weeks. There are no extremely long lived isotopes produced and the residual activity is dominated by ^{45}Ca ($T_{1/2}$ = 163 days).

The effect of operating time on the radioactivity after shutdown is illustrated in Figure 7. Shown is the total radioactivity of the blanket in the 316 SS system and the first wall activity for two and ten year operating times. The first wall initially contributes about 30% of the activity and maintains this fraction as the activity decays away. The activity of a first wall operated for two years is 80% of a first wall operated for ten years, so that replacing the first wall every two years requires handling almost as much radioactivity as would be the case for a ten year first wall lifetime.

It may be noted that after shutdown the two and ten year activity curves are initially parallel corresponding to the decay of the shorter lived isotopes which have saturated. After about two hours, the curves start to diverge slowly with the activity from the two year operation dropping off faster as expected. Even after twenty years, the two year wall still has more than 1/5 the activity of the ten year wall.

Nature of Activity

Following Steiner[3] the "Biological Hazard Potential" (BHP) has been calculated at the time of shutdown for the first wall. This quantity

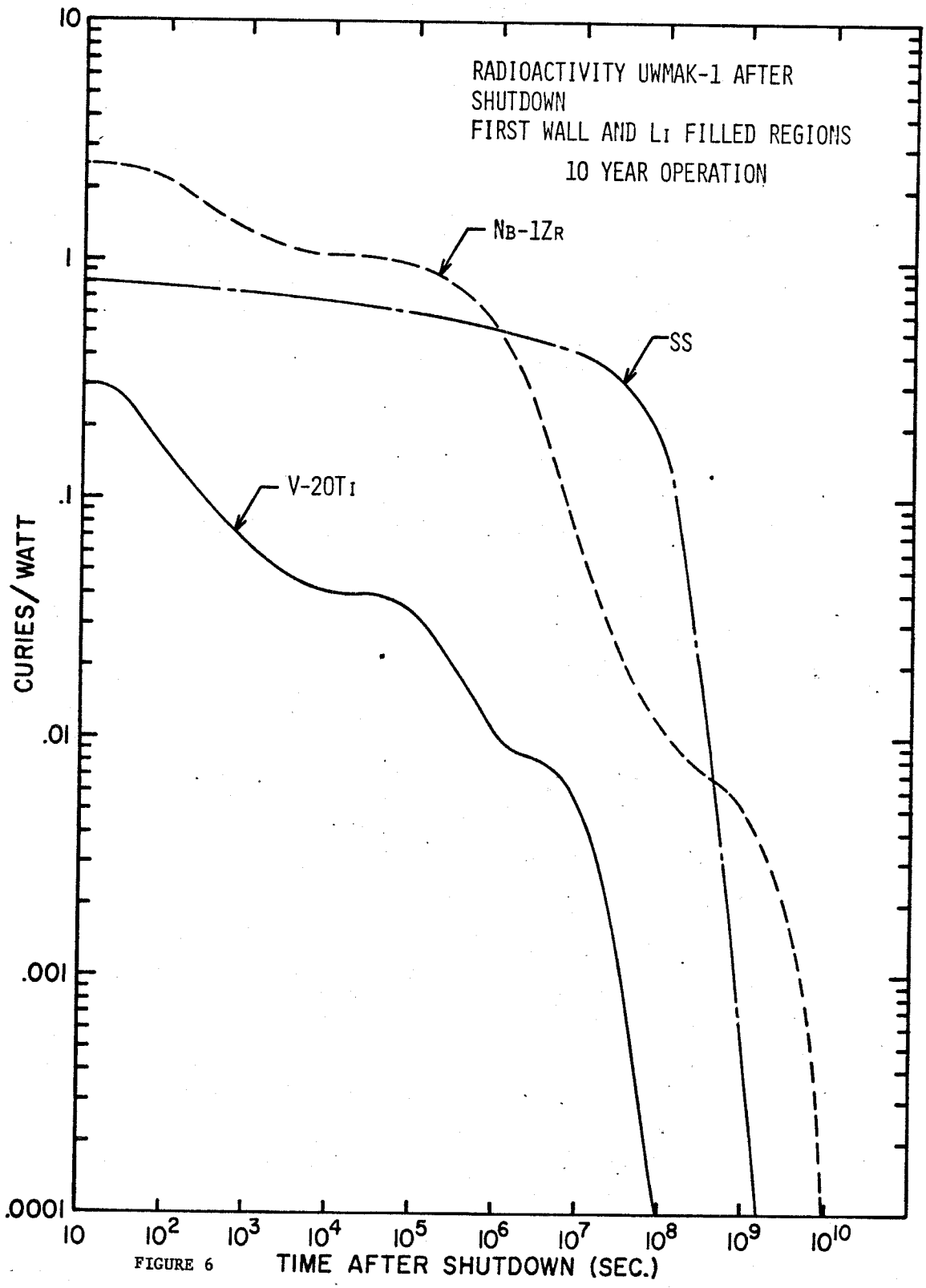
RADIOACTIVITY UWMAK-1 AFTER
SHUTDOWN
FIRST WALL AND Li FILLED REGIONS
10 YEAR OPERATION
Nb-1Zr
SS
V-20Ti
CURIES/WATT
10
1
.1
.01
.001
.0001
10
10^2
10^3
10^4
10^5
10^6
10^7
10^8
10^9
10^10
TIME AFTER SHUTDOWN (SEC.)

FIGURE 6

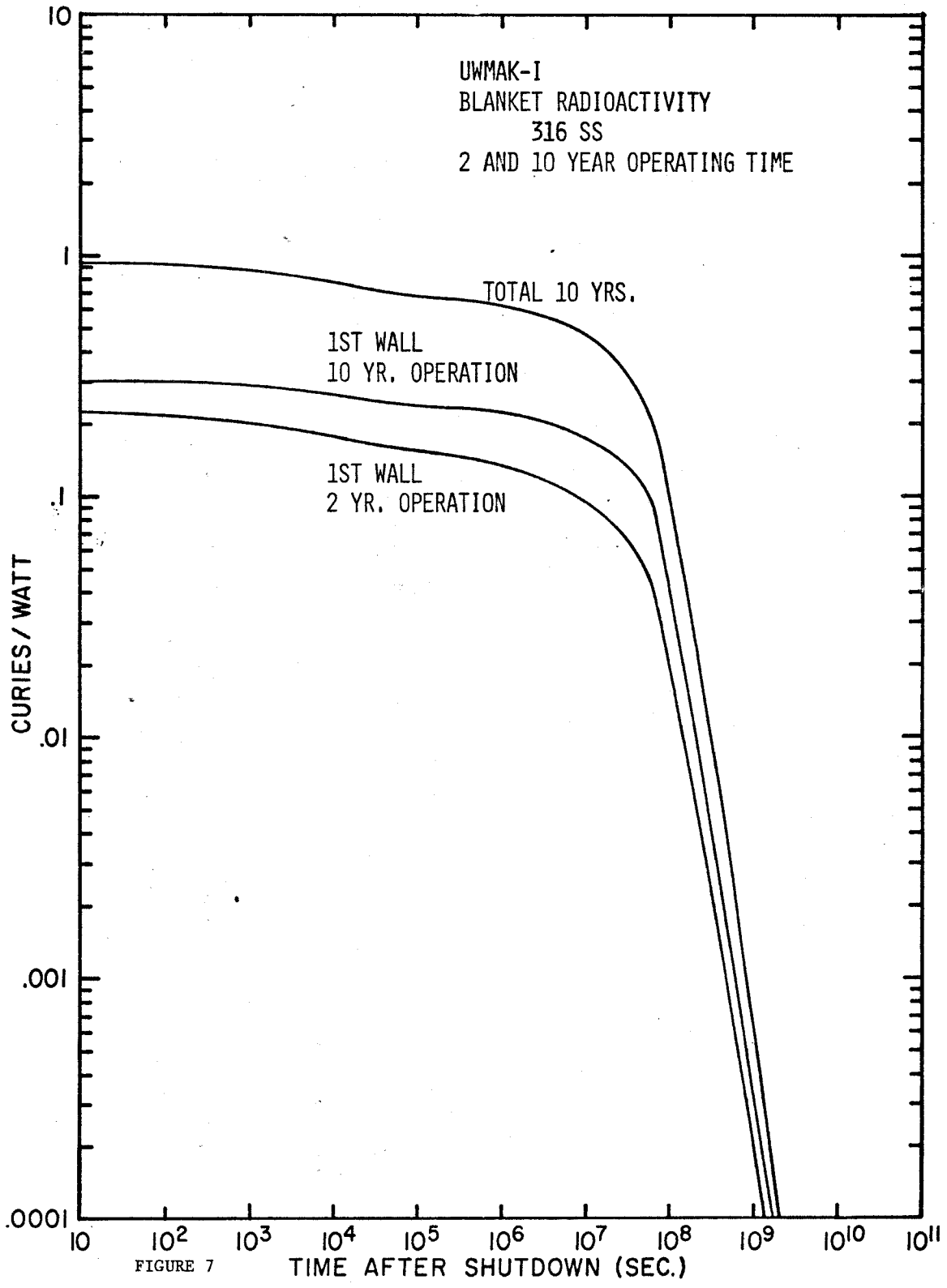
UWMAK-I
BLANKET RADIOACTIVITY
316 SS
2 AND 10 YEAR OPERATING TIME
TOTAL 10 YRS.
1ST WALL
10 YR. OPERATION
1ST WALL
2 YR. OPERATION
CURIES / WATT
10
1
.1
.01
.001
.0001
10
10^2
10^3
10^4
10^5
10^6
10^7
10^8
10^9
10^10
10^11
TIME AFTER SHUTDOWN (SEC.)

FIGURE 7

which is the activity in curies/kw_{th} divided by the lowest maximum permissible concentration (MPC) for general public exposure in curies/km^3 of air as taken from the AEC "Standards for Protection Against Radiation." The BHP is equivalent to the volume of air required to dilute the activity per thermal kilowatt to MPC. It provides a convenient way of making realtive comparisons between systems taking into account the biological effects of the radioactivty. Table V presents the BHP for the isotopes making a significant contribution for all three systems. To put these values in persepctive, the values from an "advanced Fission Reactor" as taken from reference 3 are also shown in Table V. These values confirm that a fusion system may require the same degree of radiation protection as a fission system in the short time after an as yet undefined catastrophic accident.

It is interesting to note that over 80% of the activity in 316 SS comes from five isotopes - ^{55}Fe, ^{56}Mn, ^{58}Co, ^{51}Cr, and ^{54}Mn. The activity (in curies) of these isotopes is approximately four times that of the I and Pu in fission fuel used to generate the same power. But that is not always the first measure of radioactivity hazard. The BHP of the 316 SS isotopes is 0.01 to 1% of the BHP associated with iodine and plutonium isotopes in the fission fuel. Therefore, it may be concluded that the radioactivity in UWMAK-I represents from 1/100 to 1/10,000 the radioactive hazard associated with equivalent sized fission plants.

The BHP of Nb-1Zr is much greater than that of 316 SS. The outstanding example is $^{92}Nb^m$ with a BHP of ~15,000 compared to a maximum BHP of any isotope of 316 SS of 24. However, the BHP for

Nb-92m may be too high. If a specific nuclide in 10CFR20 has not been evaluated, it is assigned an MPC value of 1×10^{-10} μc/ml of air. Nb-92m is one of these cases. It is possible that an upward revision of the MPC could occur if that isotope was evaluated. This in turn would lower the BHP, but even with a change of this sort, which is not likely to change the MPC by more than a factor of ten, it is apparent that the BHP of a Nb-1Zr wall would still be significantly greater than that of stainless steel. Finally, it is noted that a considerable amount of ^{89}Sr is produced either from the ZR which in the Nb as an alloying agent or from the Zr produced by transmutation reactions. The half life of ^{89}Sr is ~51 days, much shorter than ^{90}Sr (~28y), but its BHP is about the same. Mechanisms for release of ^{89}Sr should be investigated (i.e. corrosion, sputtering, etc.).

The BHP of the V-20Ti system is the most favorable of the three. The values are about an order of magnitude less than for 316 SS and in addition the half lives are generally shorter. Consideration of impurities or other alloying elements which may be added would alter this conclusion however.

Afterheat

A direct consequence of the generation of large amounts of radioisotopes is that they will generate heat as they decay. If this heat is not properly disposed of, it can damage reactor components and/or make maintenance on the first wall a difficult task. The afterheat in the blanket of UWMAK-I was calculated using the information on radioactivity presented in the previous section. The energies of the decay beta particles and photons are taken from reference 9. The energy of the beta particles is taken to be deposited at the site of the emission of the particle. The average energy of a beta particle

Table V

First Wall Radioactive Inventory at
Shutdown After 10 Years of Operation

Isotope	Specific Activity dps/cm^3	Activity ci/kw$_{th}$	MPC µci/ml	"Biological Hazard Potential" km^3 of air/kw$_{th}$	$t_{1/2}$
			316 SS		
V-49	1.1 x 10(6)	0.67	1 x 10(-10)	6.7	331 days
Mn-54	4.0 x 10(10)	24	1 x 10(-9)	24	313 days
Mn-56	6.9 x 10(11)	42	2 x 10(-8)	2.1	2.58 hours
Fe-55	2.3 x 10(12)	140	3 x 10(-8)	4.6	2.7 years
Co-58	4.7 x 10(11)	29	2 x 10(-9)	14.5	71.4 years
Co-60	7.7 x 10(10)	4.7	3 x 10(-10)	15.6	5.26 years
Ni-57	1.8 x 10(10)	1.1	1 x 10(-10)	11	36.1 hours
Total[(a)]		~310		~80	
			Nb-1Zr		
Nb-92m	2.5 x 10(13)	1520	1 x 10(-10)	15200	10.1 days
Nb-95m	8.1 x 10(11)	49.6	1 x 10(-10)	500	87 hours
Nb-95	6.8 x 10(11)	4.15	3 x 10(-9)	14	35.1 days
Zr-89	1.7 x 19(10)	1.02	1 x 10(-10)	10	78.4 days
Sr-89	6.20 x 10(11)	37.9	3 x 10(-10)	126	50.8 days
Total[(a)]		~1900		~16000	
			V-20Ti		
Ca-45	4.2 x 10(10)	2.58	1 x 10(-9)	2.6	165 days
Sc-46	3.1 x 10(10)	1.87	8 x 10(-10)	2.3	83.8 days
Sc-48	2.99 x 19(10)	12.1	5 x 10(-9)	2.5	1.82 days
Ti-45	1.90 x 10(9)	0.12	1 x 10(-10)	1.9	3.08 hours
Total[(a)]		~56		~9	
		Advanced Fission Reactor (Ref. 5)			
I-131		31.6		330	8 days
I-131 (milk pathway)		31.6		230,000	
Pu-239		0.06		1,000	24,400 years
Total Plutonium Isotopes		18.2		8,300	

(a) Including those isotopes not listed here

is calculated as described in reference 1 rather than assuming a constant fraction of the maximum energy e.g. 30% as has been done in earlier work. For simplification, the gammas were also assumed to deposit all of their energy in the immediate vicinity of the origin of the radiation. An examination of the mean free path of a typical decay gamma shows that this is not a good assumption and the energy of the gammas will likely not be deposited near the point of emission. However, this assumption is probably conservative in the sense that the largest source of gammas is the first wall and if the gammas which originate there do not deposit their energy in the first wall, then the decay heat there will be somewhat less than calculated.

Time Dependence of Afterheat Generation

Many of the features exhibited by the induced radioactivity show up in the afterheat also. However, the different decay energies of the various isotopes introduce significant changes in the shape and relative magnitudes to the results. Figure 8 shows the build up of the total afterheat of shutdown in the blanket for the three systems as a function of operating time prior to shutdown. Here, as with the radioactivity, a rather rapid build up of afterheat occurs initially. Concentrating on 316 SS, it is seen that after only 17 hours of operation, the afterheat is almost 50% of the thirty year value. This behavior is again due to the saturation of the short lived isotopes which, in this case, have the more energetic decay products.

The afterheat in the Nb-1Zr system shows a somewhat slower initial rise and by ~10 weeks, the afterheat of the Nb-1Zr and 316 SS systems are the same. The Nb-1Zr afterheat remains less than that of 316 SS until

FIG. 8

Afterheat at Shutdown
as a Function of Operating Time
UWMAK-I

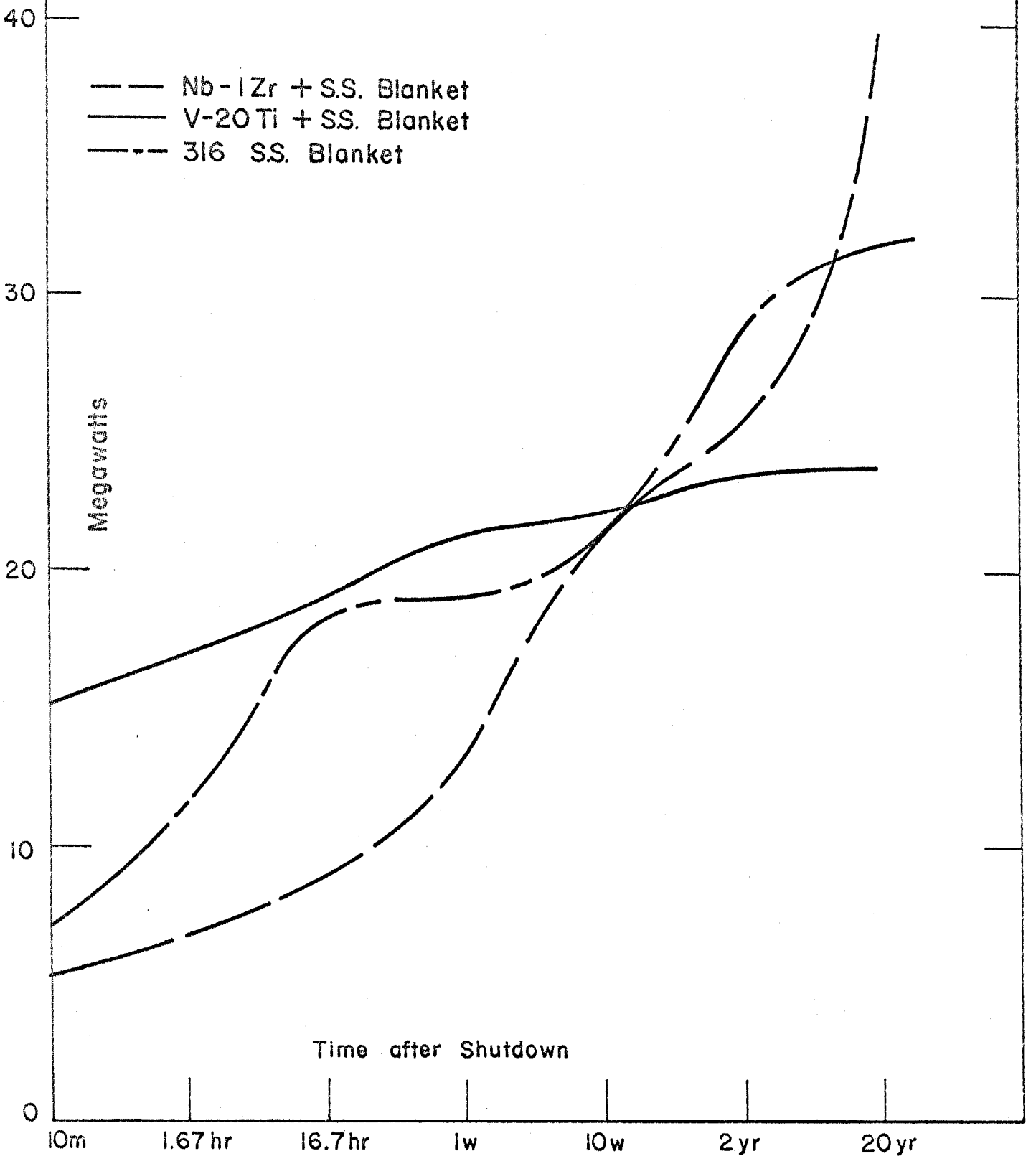

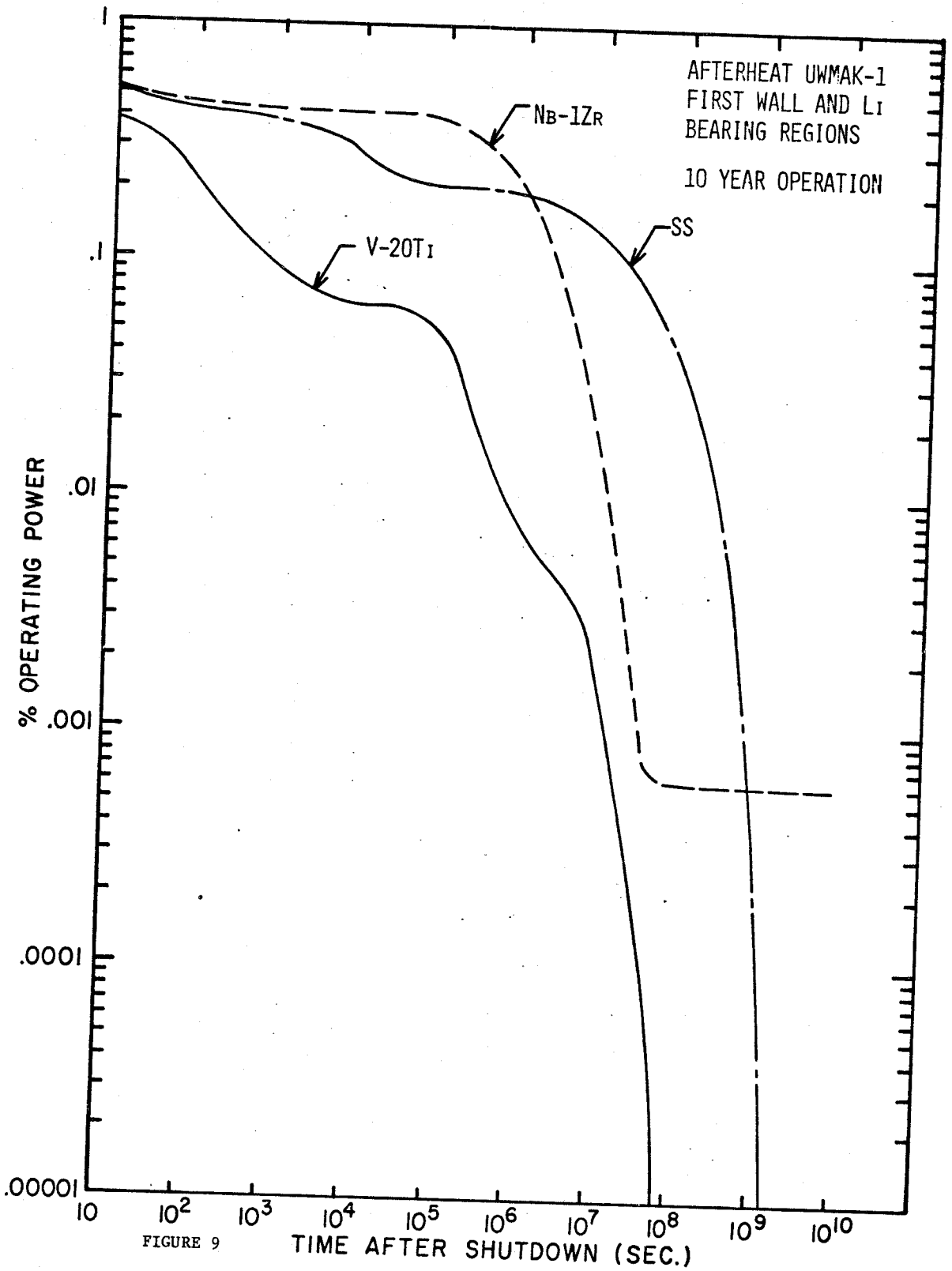
AFTERHEAT UWMAK-1
FIRST WALL AND LI
BEARING REGIONS
10 YEAR OPERATION
NB-1ZR
SS
V-20TI
% OPERATING POWER
1
.1
.01
.001
.0001
.00001
10
10^2
10^3
10^4
10^5
10^6
10^7
10^8
10^9
10^10
TIME AFTER SHUTDOWN (SEC.)

FIGURE 9

~5 years of operation after which time it continues to increase while that of 316 SS shows signs of saturation. The afterheat from V-20Ti on the other hand has a much more rapid initial rise followed by a relatively slow increase showing definite saturation. The change in afterheat from 10 minute operation to 20 years of operation is less than a factor of two.

Time Dependence of Afterheat Following Shutdown

Figure 9 shows the afterheat of the lithium bearing region following shutdown again for a 10 year operating time. The afterheat is presented as percent of operating power. The afterheat from the 316 SS system is initially ~0.5% and, as with the radioactivity, the initial drop is rather slow requiring about two years to reduce the radioactivity by a factor of ten. Nb-1Zr has very nearly the same initial afterheat for this same operating time. The initial decay for the first few days is even slower than for 316 SS. The decay after this time is more rapid than in 316 SS requiring only ~10 weeks to be down by a factor of ten. At long times (>two years) however, the presence of long lived ^{94}Nb leads to an almost constant afterheat, greater than that of 316 SS.

The V-20Ti alloy, because of the absence of long lived isotopes, presents a more favorable case. The initial afterheat is less, ~0.4% compared to ~0.6% for SS, and the initial decay is much more rapid requiring only about one day to be reduced by a factor of ten. The subsequent decay is somewhat slower due primarily, as with the case of the radioactivity, to the presence of ^{45}Ca ($T_{1/2}$ = 163 days) produced from the titanium. Even so, the afterheat is down by about five orders of magnitude after only two years.

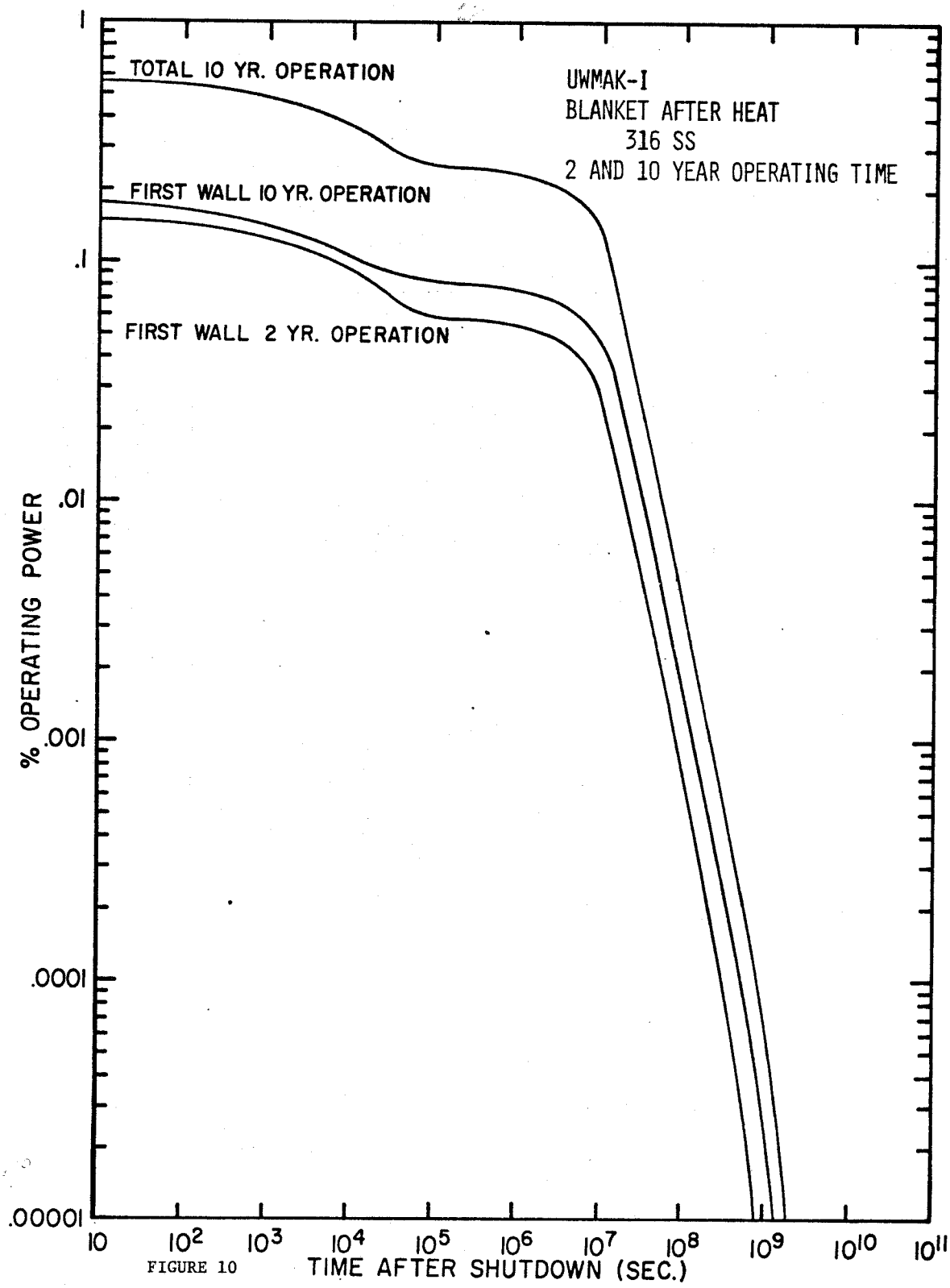
TOTAL 10 YR. OPERATION
FIRST WALL 10 YR. OPERATION
FIRST WALL 2 YR. OPERATION
UWMAK-I
BLANKET AFTER HEAT
316 SS
2 AND 10 YEAR OPERATING TIME
% OPERATING POWER
1
.1
.01
.001
.0001
.00001
10
10^2
10^3
10^4
10^5
10^6
10^7
10^8
10^9
10^10
10^11
TIME AFTER SHUTDOWN (SEC.)

FIGURE 10

The effect of operating time on the decay of the afterheat following shutdown is shown in Figure 10. The total afterheat of the blanket is compared with the first wall afterheat for two and ten year operating times. The first wall contributes ~25% of the initial afterheat and maintains this fraction. A 316 SS first wall operating for two years has an initial afterheat ~90% that of a first wall operated for 10 years.

Comparison of Fusion and Fission Systems

Reference was made in an earlier section to the BHP of a fusion system compared to that of an "Advanced Fission System". Since fusion systems have often been advanced as offering the possibility of providing "clean" power it is of interest to make a comparison of the two systems to examine quantitative differecnes. The LMFBR treated in a study from the Oak Ridge National Laboratory will be used[11] as a reference fission system. In this study, calculations have been made of the activity and afterheat of fission products, fuel cladding and activities for an LMFBR with a fuel exposure of 1.4 years. Figure 11 shows a comparison of the activity following shutdown of the fusion or fission reactor. It is seen that the activity of the fission system at shutdown is primarily due to the fission products and the actinides. Both the cladding and the sodium coolant make a small contribution. The activity of the UWMAK-I is primarily due to the activation of the structure. After a decay period of ~6 months, the activity of the fusion reactor is larger than the fission plant. At times longer than 10 years, however the activity of UWMAK-I is lower because of the absence of very long lived isotopes. Thus, the fusion

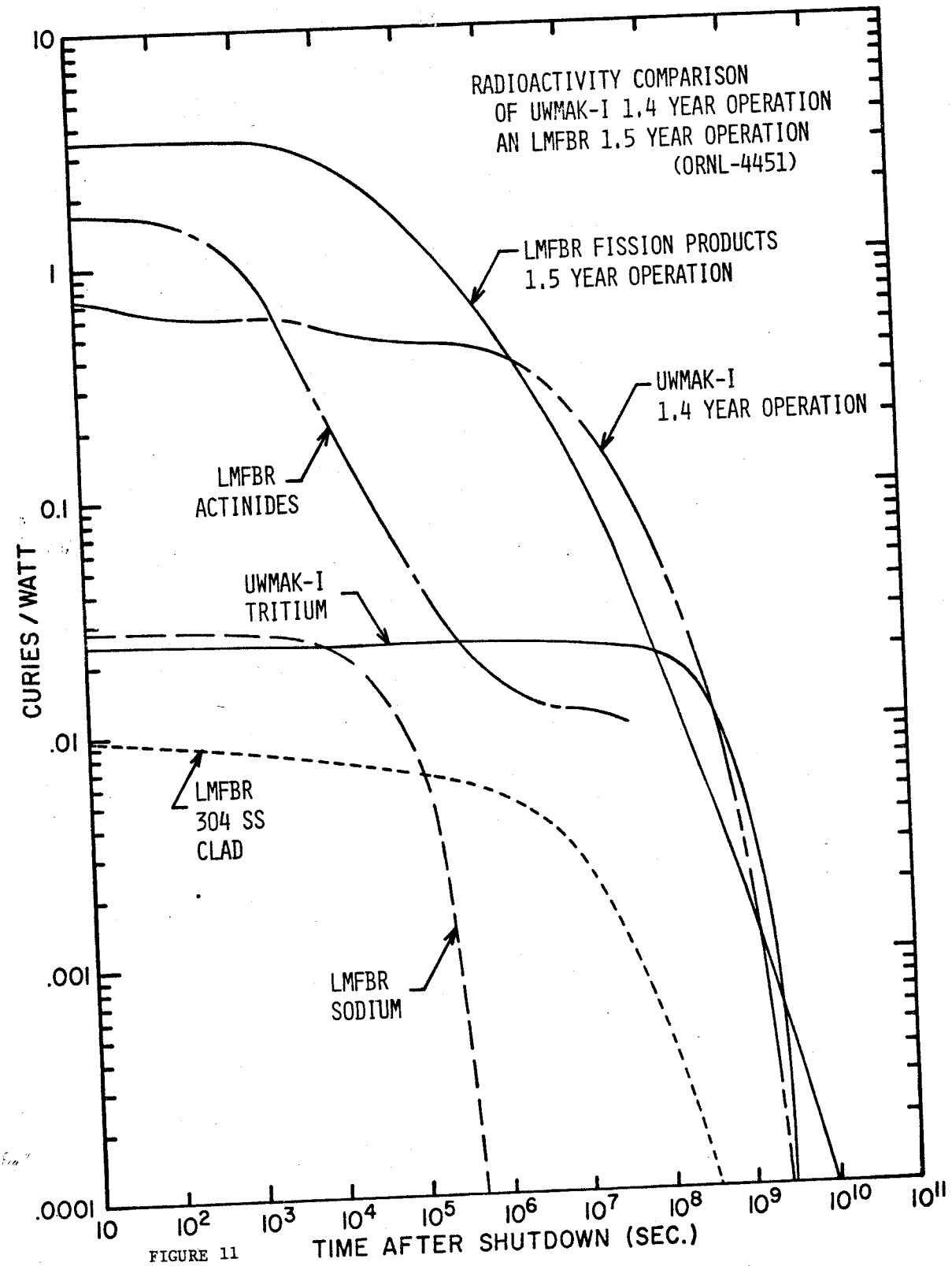
RADIOACTIVITY COMPARISON
OF UWMAK-I 1.4 YEAR OPERATION
AN LMFBR 1.5 YEAR OPERATION
(ORNL-4451)
LMFBR FISSION PRODUCTS
1.5 YEAR OPERATION
UWMAK-I
1.4 YEAR OPERATION
LMFBR
ACTINIDES
UWMAK-I
TRITIUM
LMFBR
304 SS
CLAD
LMFBR
SODIUM
CURIES / WATT
10
1
0.1
.01
.001
.0001
10
10²
10³
10⁴
10⁵
10⁶
10⁷
10⁸
10⁹
10¹⁰
10¹¹
TIME AFTER SHUTDOWN (SEC.)

FIGURE 11

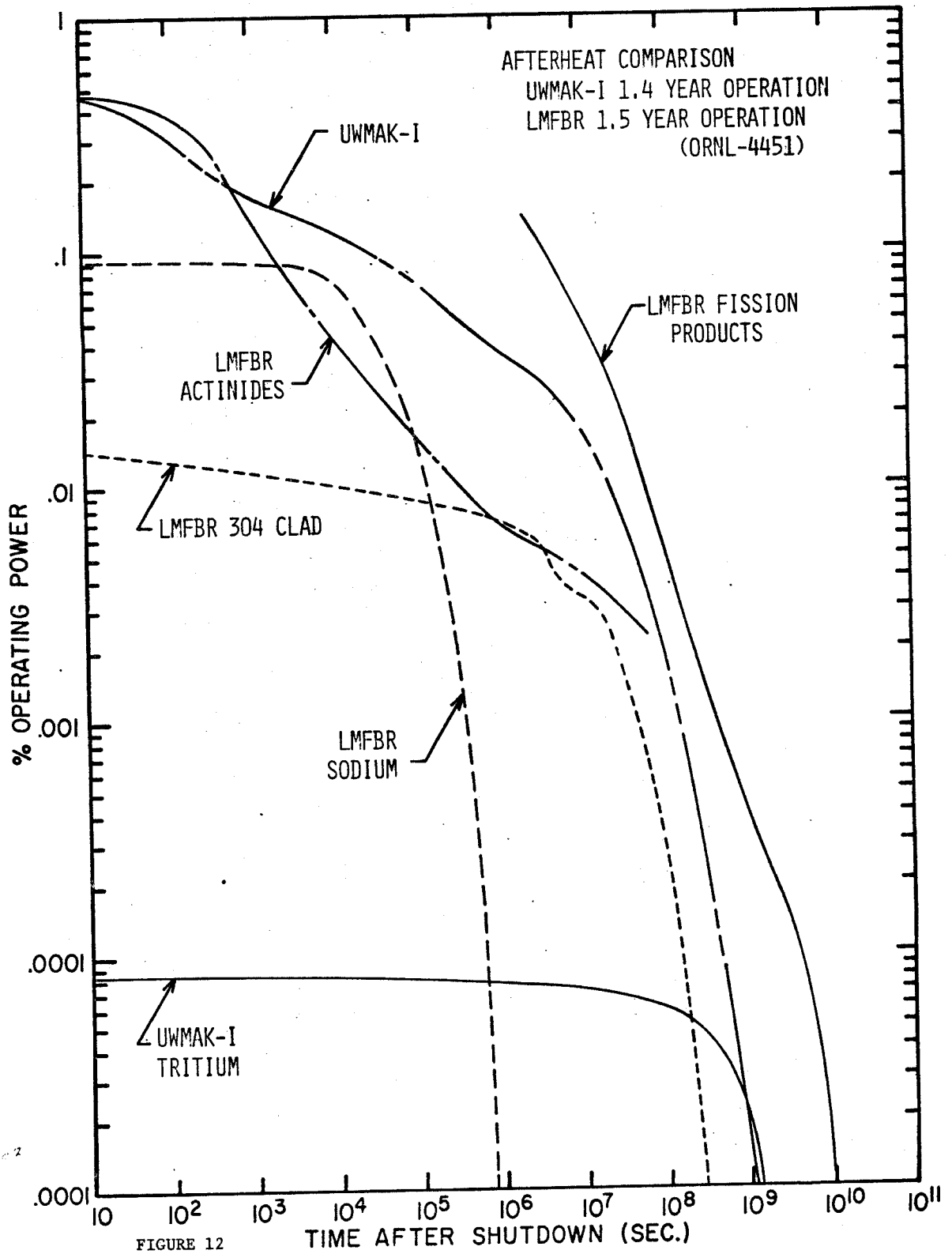
AFTERHEAT COMPARISON
UWMAK-I 1.4 YEAR OPERATION
LMFBR 1.5 YEAR OPERATION
(ORNL-4451)
UWMAK-I
LMFBR FISSION PRODUCTS
LMFBR ACTINIDES
LMFBR 304 CLAD
LMFBR SODIUM
UWMAK-I TRITIUM
% OPERATING POWER
1
.1
.01
.001
.0001
.0001
10
10^2
10^3
10^4
10^5
10^6
10^7
10^8
10^9
10^10
10^11
TIME AFTER SHUTDOWN (SEC.)

FIGURE 12

reactor has an advantage at both short and long times but in the period 1-100 years both systems have comparable activities. It should be noted, however, that this analysis does not factor in the biological effects which, as was seen earlier, can have a significant effect on the evaluation of the two systems. Note that the tritium activity (based on a 10 kg inventory) is only about 3% of the total activity at shutdown it becomes comparable to the structure activity after about 20 years. The decay is sufficiently rapid, however, it presents no long term problem.

Figure 12 shows the afterheat for the same systems. At shutdown, the afterheat of the UWMAK-I is about the same as that produced by the actinides in the fission system. Although no values are given in reference 11 for the afterheat of fission products for the first few days after shutdown, previous experience with light water systems[3] would suggest that the afterheat is approximately an order of magnitude greater than the UWMAK-I structure i.e. ~5% of the operating power. It is seen that the afterheat of the fusion plant is less than that of the fission plant at shutdown and remains so at all times. At long times, the advantage of the fusion reactor in this regard is especially apparent even if the afterheat of the actinides is disregarded. Because of the low beta energy associated with tritium decay, the contribution of the afterheat from the coolant itself is insignificant. Another important point in this respect is that the energy density of CTR systems is much lower than in the more compact fission reactors.

In summary, it appears that a fusion reactor as typified by UWMAK-I offers a real advantage in radioactivity and afterheat immediately following shutdown compared to fission reactors. At intermediate times

the advantage is less pronounced whereas at long times in UWMAK-I the radioactivity and afterheat are significantly lower than the fission system.

Acknowledgement

This work was supported by the Wisconsin Utilities Research Foundation and the United States Atomic Energy Commission.

Figure Captions

1. University of Wisconsin CTR (UWMAK-I) Blanket, Shield and Magnet Structure as Used for Radioactivity and Afterheat Calculations.

2. UWMAK-I Neutron Spectrum at the First Wall Compared with FFTF and EBR-II Core Center Spectra.

3. Buildup of Helium in UWMAK-I from the $^{58}Ni(n,\gamma)$ $^{59}Ni(n,\alpha)$ Reaction.

4. Helium Buildup in UWMAK-I for 316 SS, Nb-1Zr, and V-20Ti First Wall Materails.

5. Radioactivity at Shutdown in UWMAK-I for 316 SS, Nb-1Zr and V-20Ti Systems Versus Operating Time.

6. Decay of Radioactivity Following Shutdown of UWMAK-I for a Ten Year Operating Time. First Wall and Lithium Bearing Regions Only. The Tritium Contribution is not Considered.

7. Decay of Total and First Wall Radioactivity of UWMAK-I for Two and Ten Year Operating Times. 316 SS Structure. The Tritium Contribution is not Considered.

8. Afterheat at Shutdown in UWMAK-I for 316 SS, Nb-1Zr and V-20Ti Systems Versus Operating Time.

9. Decay of Afterheat Following Shutdown of UWMAK-I for a Ten Year Operating Time. First Wall and Lithium Bearing Regions Only. The Tritium Contribution is not Included.

10. Decay of Total and First Wall Afterheat in UWMAK-I for Two and Ten Year Operating Times. 316 SS Structure. The Tritium Contribution is not Considered.

11. Comparison of Radioactivity of UWMAK-I and an LMFBR (ref. 10). The Operating Time is ~1.5 years.

12. Comparison of the Afterheat from UWMAK-I and an LMFBR (ref. 10). The Operating Time is ~1.5 years.

References

1. B. Badger et al., UWMAK-I - A Wisconsin Toroidal Fusion Reactor Design - University of Wisconsin Fusion Design Memo-68, September 17, 1973.

2. G. L. Kulcinski, R. G. Brown, R. G. Lott and P. A. Sanger, "Radiation Damage Limitations in the Design of the Wisconsin Tokamak Fusion Reactor," to be published in this issue.

3. D. Steiner and A. P. Fraas, Preliminary Observations on the Radiological Implications of Fusion Power, Nuclear Safety, 13, 353 (1972).

4. M. A. Abdou, C. W. Maynard and R. Q. Wright, MACK: A Program to Calculate Neutron Energy Release Parameters (Fluence-to-Kerma) and Multigroup Neutron Reaction Cross Sections from Nuclear Data in ENDF Format, University of Wisconsin Fusion Design Memo-37.

5. e.g. Nuclear Data, Academic Press, New York, N.Y.

6. F. T. Sisco and E. Epremian, Columbium and Tantalum, New York John Wiley and Sons, Inc.

7. M. Hansen, Constitution of Binary Alloys 2nd Edition, McGraw Hill, New York, (1958).

8. G. J. Kirouac, Calculated Thermal (n,α) Cross Section for Nickel 59, Nucl. Sci. Eng. 46, 427 (1971). See also H. M. Eidland and G. J. Kirouac, Measurements of the ^{59}Ni (n,α) Cross Section for Thermal Neutrons, to be published.

9. Code of Federal Regulations, Title 10, Part 20, "Standards for Protection Against Radiation," USAEC, Washington, D.C.

10. C. M. Lederer, J. M. Hollander and I. Perlman, Table of Isotopes 6th Edition, Wiley, New York, (1967).

11. Chemical Technology Division, ORNL, "Siting of Fuel Reprocessing and Waste Management Facilities, "ORNL-4451 (July 1971); USAEC Clearinghouse for Federal Scientific and Technical Information, Springfield, Virginia 22151.